Distributed Automatic Generation Control For Multi Area Power System

[1]Bandari Rajkumar, [2]Thumula Venugopal,
[2]Associate professor,
[1]Electrical and Electronics Engineering,
[1]Vaagdevi College of Engineering, Warangal, India

Abstract : Automatic generation control(AGC) is one of the most critical issues in multi area power system control. AGC models encounters many problems like imbalance between generation and load demand, data exchanging, calculation complexities and memory requirements. To overcome such difficulties this paper presents a controller based on multi agent system (MAS). Change in communication topology, time delay , network induced effects are used to test the system performance. a controller design based on reinforcement learning and it has two individual agents namely controller agent and estimator agent. for the tuning of input parameter particle swarm optimization is used. Furthermore, controller design and control scheme are described. Mean square error of different states of the power system are analyzed in addition. The simulation results shows the capability of proposed controller for distributed automatic generation control in multi area power system.

IndexTerms **- Communication topology (CT), Automatic Generation Control (AGC), multi-agent reinforcement learning (MARL), smart grid (SG)**

I. INTRODUCTION

Load frequency control is to make balance between power generation and demand in addition to losses. The losses occurring due to delay in communication network. In general networks suffering with data transmission, computing and storage problems .by making decentralization of system ,the performance could be improved compared to classical centralized system. Smart grids are becoming more reliable with these data communication systems. The power system mainly based on the algorithms for its operational and control techniques. Inter connected networks with their bi directional data flow make communication mor effective and feasible and it ensures balancing of generation and demand.

Significance of load frequency control monitoring is exponentially increasing. Multiple configurations of power system models with control strategies discussed in both centralized and distributed LFC system [1], importance of distributed LFC for efficient communication in interconnected system is addressed. Effect on stability with communication losses is explained in[2], LFC base d time delay estimation and packet loss with markovian technique is presented in [3], smart grid and its interaction effects on the information and communication technology in data centers is presented with reduction in maintenance cost energy efficient management in communication systems is also presented [4].A time varying communication topology matrix is used to observe the changes in smart grid with communication losses in[5], and a LFC strategy with distributed gain scheduling is proposed to reduce the losses due to change in communication model. Communication delay impact on the power system dynamic performance addressed for minimum deviation of frequency parameter is investigated in [6]. Network induced effects, time varying delays, packet losses and data disorder in wide area power system control is explained [7].

I. MODELING OF A POWER SYSTEM IN SMART GRID

The basic objective of LFC in integrated power system area is to require the balancing between of total generation against total load demand, including system losses and maintain a tie line power at a scheduled value. The AGC via communication network in a SG is shown in Fig. 1.The power system dynamics is modeled as a continuous-time simulation while communication network as a discrete event due to its inherent nature. The information for frequency deviation of each area and tie-line power between two areas is transmitted via communication network through local/control center, to each area for respective control action. The state-space modeling of thermal power system is presented.

In LFC problem, our aim is to keep the frequency close to its nominal value by adjusting the balance between generation set point and load demand. The frequency deviation of each area is governed by

$$\Delta \dot{f}_i = -\frac{1}{T_{pi}}\Delta f_i + \frac{K_{pi}}{T_{pi}}\Delta P_{ti} - \frac{K_{pi}}{T_{pi}}\Delta {P_{tie}}^{i} - \frac{K_{pi}}{T_{pi}}\Delta P_{Di} \qquad (1)$$

Where $\Delta \dot{f}_i$ is the frequency deviation of individual area,ΔP_{ti} is the generator mechanical power deviation, $\Delta {P_{tie}}^{i}$ is the tie line power deviation of between two areas, ΔP_{Di} is the load deviation of each unit, 1

$\frac{1}{K_{pi}} = D_i$ is the damping coefficient of each area, and T_{pi}

$\frac{T_{pi}}{K_{pi}} = Mi$ is the equivalent inertia of each area.

The turbine dynamics is represented as

$$\Delta \dot{P_{ti}} = -\frac{1}{T_{pi}}\Delta P_{ti} + \frac{1}{T_{ti}}\Delta P_{gi} \quad (2)$$

Where T_{ti} is the turbine constant of each area and ΔP_{gi} is the turbine valve position deviation of each area.

The governor equation is given by

$$\Delta \dot{P_{gi}} = -\frac{1}{R_i T_{gi}}\Delta f_i - \frac{1}{T_{gi}}\Delta P_{gi} + \frac{1}{T_{gi}}\Delta P_{ri} \quad (3)$$

Where R_i is the droop coefficient of individual area and ΔP_{ri} is the load generation balance point.

The net tie-line deviation between two different areas is represented as

$$\Delta {P_{tie}}^{i} = \sum_{j=1,j\neq i}^{N} 2\pi T_{ij}(\Delta f_i - \Delta f_j) \quad (4)$$

WhereT_{ij} is the synchronization coefficient, Δf_i is the frequency deviation of area j, and N is the total number of interconnected areas.

The state-space modeling of i th area is given by

$$\dot{x_i} = A_{ii}x_i + B_{ii}u_i \sum_{j=1,j\neq i}^{N} A_{ij}x_j + T_i\Delta P_{di} \quad (5)$$

Where $x_i = [\Delta f_i\ \Delta P_{ti}\ \Delta P_{gi}\ \Delta {P_{tie}}^{ij}]^T$, $u_i = \Delta P_{ri}$

$$A_{ii} = \begin{bmatrix} -\frac{1}{T_{pi}} & \frac{K_{pi}}{T_{pi}} & 0 & -\frac{K_{pi}}{T_{pi}} \\ 0 & -\frac{1}{T_{ti}} & \frac{1}{T_{ti}} & 0 \\ -\frac{1}{R_i T_{gi}} & 0 & -\frac{1}{T_{gi}} & 0 \\ \sum_{j=1,j\neq i}^{N} 2\pi T_{ij} & 0 & 0 & 0 \end{bmatrix}$$

$$A_{ij} = \begin{bmatrix} 0 & 0 & 0 & 0 \\ 0 & 0 & 0 & 0 \\ 0 & 0 & 0 & 0 \\ -2\pi T_{ij} & 0 & 0 & 0 \end{bmatrix}$$

$$B_i = \begin{bmatrix} 0 & 0 & \frac{1}{T_{gi}} & 0 \end{bmatrix}^T \quad T_i = \begin{bmatrix} -\frac{1}{M_i} & 0 & 0 & 0 \end{bmatrix}^T .$$

In simulation study, the initial condition of frequency deviation for all the four areas is assumed as 0.5 Hz, while the initial conditions of other states as zero. Aii ,Bi ,ui , T_i , and ΔPdi are system matrix, system input, control input matrix, disturbance, and load disturbance of i th area, respectively, whereas Aij represents the system matrix of interconnected areas. If communication infrastructure is completely reliable, the control inputs of controller can be given as

$$u_i = -K_i x_i - \sum_{j=1,j\neq i}^{N} K_{ij}x_{ij} \ , i \in \{1 \ldots . N\} \quad (6)$$

where *Ki* ,*Kij* are the controller gains obtained from the PSO algorithm. So, communication matrix can be defined as

$$C(t) = [C_{ij}\ (t)]_{N\times N} \ . \quad (7)$$

Next, diagonal elements of *C*(*t*) will always be 1, indicating communication channel for diagonal elements is always ON. Furthermore, the power system dynamics including CT is given as

$$\dot{x_i} = A_{ii}x_i + B_{ii}u_i \sum_{j=1,j\neq i}^{N} c_{ij}A_{ij}x_j + T_i\Delta P_{di} \quad (8)$$

$$u_i = -K_i x_i - \sum_{j=1,j\neq i}^{N} c_{ij}K_{ij}x_{ij} \ , i \in \{1 \ldots . N\}. \quad (9)$$

Putting the value of u_i in (8), the closed-loop dynamics of the system can be represented as

$$\dot{x_i} = \hat{A}_{ii}x_i + B_{ii}u_i \sum_{j=1,j\neq i}^{N} c_{ij}\hat{A}_{ij}x_j + T_i\Delta P_{di} \ . \quad (10)$$

Often, communication structure modeling refers to the reconstruction of state and/or output specific paths, but if the structure to be modeled is subject to large uncertainties, it is better to include several topologies of structure rather than the exact path. Mainly, these topologies are based on a multimodal representation of the structure, because of the large degree of uncertainty in the establishment of communication link. The one possible illustration of CT of power system is shown in Fig. 2(a).

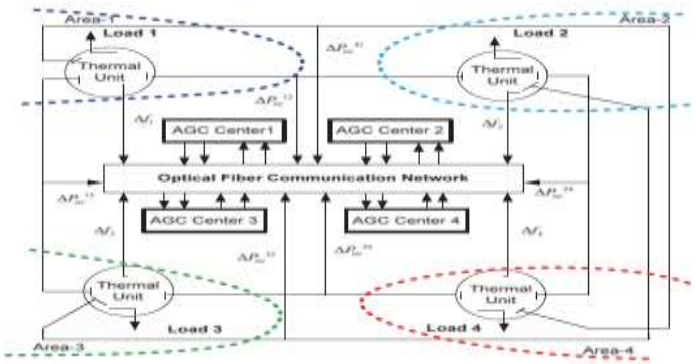

Fig. 1. Framework structure of a multi-area power system having communication network

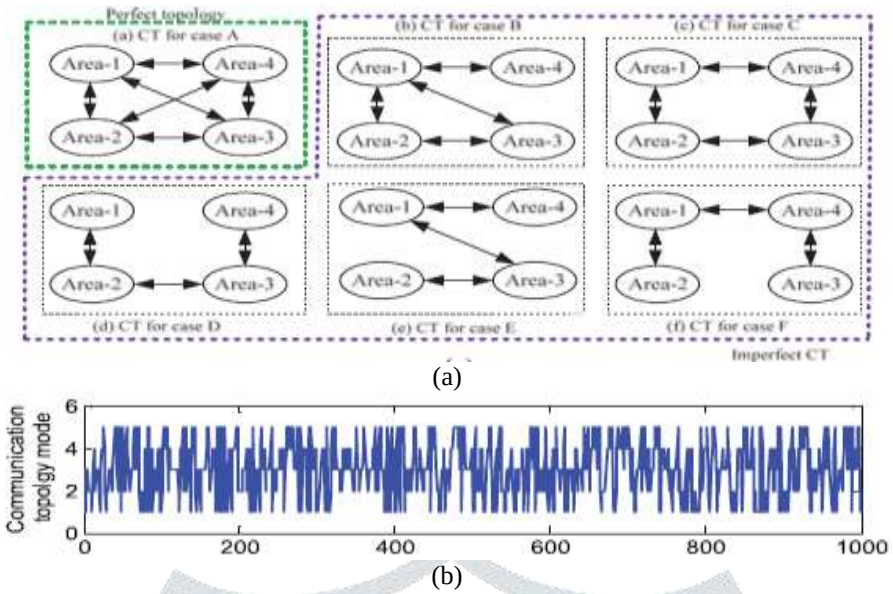

Fig. 2. CTs between the agents (four areas). (a) Illustration of possible CT for multi-area power system. (b) One sample CT modes using a Markov process.

III. IMPLEMENTATION OF MARL TECHNIQUE

In this section, an MARL technique is implemented for a multi-area power system with communication network. The complex hybrid behaviors are caused due to frequent switching between different modes of CTs as the logic relation operation and operating modes of interconnected area. Therefore, interactive hybrid control strategies should be designed to effectively control the complex hybrid behaviors. The modeling of a multi-area power system with MAS is given in Fig. 3(a). From Fig. 3(a), it is clear that that MAS agent will data of multi-area power system through communication network and then send it to estimator agents. Next, estimator agents will estimate the available signal and provide average ACE signal to controller.

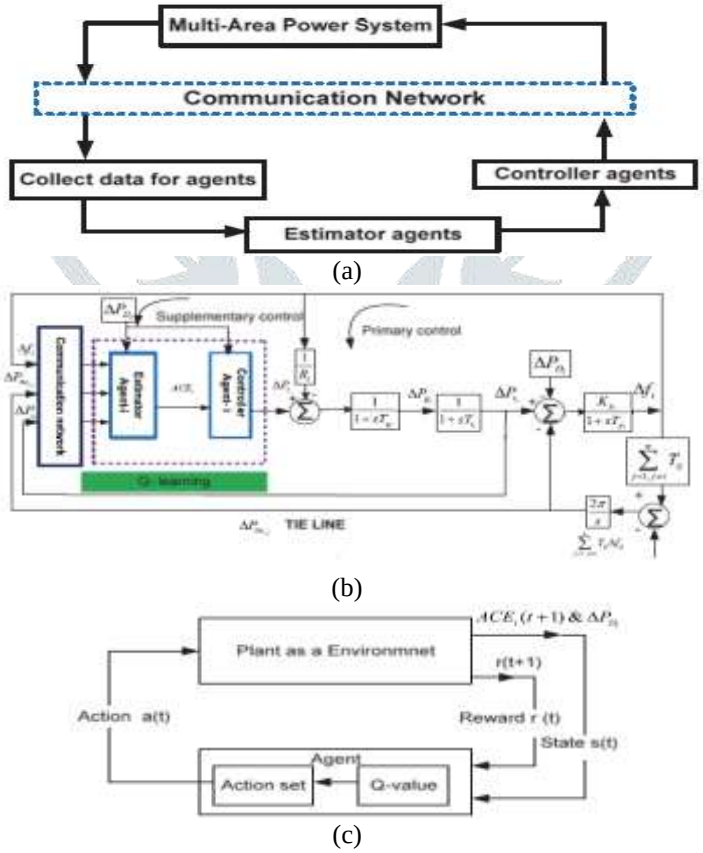

Fig. 3. Architecture for the proposed multi-area power system with communication infrastructure. (a) Flowchart of modeling of a multi-areapower system with MAS. (b) Proposed multi-agent model for *i*th area ofa thermal power system. (c) Q-learning algorithm structure

1. Multi-agent Reinforcement Learning

The main objective of an MARL technique is how to maximize the reward signal by taking some action in a particular situation. The main task of the MARL technique is to solve a problem by interacting with a system. Learner is called an agent and system that interacts with it is known as environment. Furthermore, agent will interact with environment and take the action *at* from the set of action at a time *t* s and brings the system state *st* to new system state *st* + 1. So, agent is provided with the corresponding reward signal *rt* + 1. This interaction process between agent and environment is repeated until the desired aim is achieved. In this study, a Markov decision process (MDP) is used that will contain all relevant information of state signal enabling to predict the next system state using some action with expected reward signal. Furthermore, in MDP, the aim is to maximize the sum of returned reward over time, and expected sum of discounted reward is presented by

$$R = \sum_{k=0}^{\infty} \lambda^k r_{t+k+1} \quad (11)$$

where λ is a discount factor lies between $0 < \lambda < 1$, which provides the maximum preference to recent rewards. The value function of each state is expressed as the expected reward when starting at system state *st* having following policy $\Omega(s, a)$:

$$V^{\Omega}(s) = E_{\Omega}\{\sum_{k=0}^{\infty} \lambda^k r_{t+k+1} \,|s_{t=s}\}\,. \quad (12)$$

The optimal policy of value function can be given as

$$V^{*}(s) = maxV^{\Omega}(s) \;\; \forall_s \in S. \quad (13)$$

Further action value is found using

$$Q^{\Omega}(s,a) = E_{\Omega}\{\sum_{k=0}^{\infty} \lambda^k r_{t+k+1} \,|s_t = s, a_t = a \;.\} \quad (14)$$

To find the optimal action value, Bellman's equation is used and given as

$$Q^{*}(s,a) = maxE_{\Omega}\{\sum_{k=0}^{\infty} r_{t+1} \lambda max\, Q^{*}(s_{t+1}, a') | s_t = s, a_t = a \;\}. \quad (15)$$

Next, a temporal difference method is used which learns the model of system under control. The only information available is the expected reward for each action taken for transition of state *St* to new state S*t* + 1. This algorithm, called Q-learning, will approximate the *Q*-value function. The structure of Q-learning algorithm is given in Fig. 3(c). The detail of learning process of controller is shown in Fig. 3(d). In next section, proposed control formulation is presented.

2. Proposed Control Formulation

A) Controller Agent: Conventional PI control in LFC problem may be replaced by intelligent controller for improvement in frequency deviation. In this regard, the design of LFC problem operates in discrete mode and performance of system is more flexible. Furthermore, at every time step (*k* = 1, 2, 3.....), the controller agent observe the current state of system s_k and take an action a_k in order to bring the new state of system. It is already described in above section (see Fig. 3(b)) that ACE and ΔP_D signals are available as state vector for every LFC execution period and used as input to the controller agent. It is assumed that all possible states are finite. Here, a PSO algorithm is used to compute discretized state vector value. In this paper, an RL algorithm is used to estimate the Q^*- value function and optimal policy.

Let us take a sequence of sample or training set (s_k , s_k + 1, a_k , r), where (k = 1, 2, 3.....) is LFC execution period. For each sample, transition of state s_k to new state s_k + 1 requires some action a_k , where $r_k = f(s_k , s_k + 1, a_k)$ is called a consequent reinforcement. For estimating of Q^*-value function, above sequence is used in simulation. Let us assume that for kth iteration, Q^k is the estimate of Q^*. So Q^k + 1 can be obtained as follows:

$$Q^{k+1}(s_k, \alpha_k) = Q^k(s_k, \alpha_k) + \alpha\left[g(s_k, s_{k+1}, \alpha_k) + \lambda^{max}_{\alpha \in A} Q^k(s_{k+1}, \alpha^*) - Q^k(s_k, \alpha_k)\right] \quad (16)$$

where $0 < \alpha < 1$ is constant referred as step size of the learning algorithm. In this algorithm, exploration probability for selection action for different state is used. Each state action is selected on the probability distribution over action space. Furthermore, *Q*-value is used as an objective function for the PSO algorithm. The *Q*-value of each particle insures the performance of particle for controlling the system. The learning of controller proceeds to a new generation until a predefine stop criteria is achieved. The parameters of PSO include population size = 100, maximum generation = 100, cognitive coefficient (*C*1 = *C*2 = 1.2), and inertia weight (*W* = 0.3). The simulated results using PSO of area-1 for four-area power system is shown in Fig. 4(a).

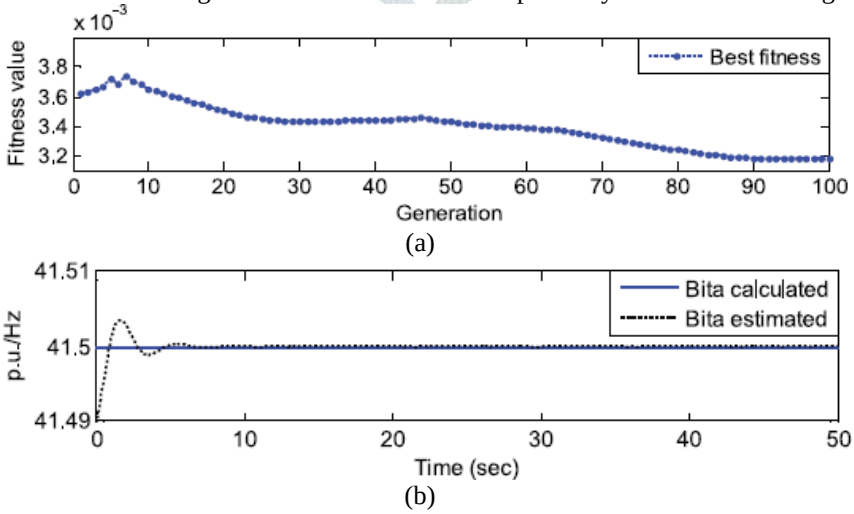

Fig. 4. Fitness value versus generation and estimation of β value:
(a) Fitness value versus generation for PSO algorithm of area-1.

(b) Estimation of β value with calculated over 50 s.

B) Estimator Agent: The ACE of system can be represented as a linear combination of tie-line power and frequency deviation of each area given by

$$ACE_t(t) = B_t \Delta f_t(t) + \Delta P_{tie(i,j)}). \qquad (17)$$

To determine the ACE, it is obvious to know the frequency bias coefficient (β). Conventionally, the value of β is usually considered as −10B, i.e., a constant value. Thus, the ACE signal will only react to internal disturbance, not to the external disturbance. Furthermore, to improve the dynamic performance of the system, the estimator agent will estimate the β parameters and determine the ACE signal accordingly. It is clear that for each LFC execution period, estimator agent will receive $\Delta P_{tiei\text{-}j}$,Δf_i , ΔP_{ti} , and ΔP_{Di} signals as inputs, then determine the β parameter, the ACE signal, and feed to the controller [see Fig. 3(b)]. The power balance of system (p.u.). for *i*th area can be represented a

$$\sum_{j=1}^{n} \Delta P_{tji}(t) - \Delta P_{Di}(t) - \Delta P_{tie_{i-j}}(t) = \frac{T_{pi}}{K_{pi}} \Delta f_i(t) + \frac{1}{K_{pi}} \Delta f_i(t). \qquad (18)$$

By using (17) and (18), we can obtain

$$\sum_{j=1}^{n} \Delta P_{tji}(t) - \Delta P_{Di}(t) + \beta_i \Delta f_i(t) - ACE_i(t) = \frac{T_{pi}}{K_{pi}} \Delta f_i(t) + \frac{1}{K_{pi}} \Delta f_i(t). \qquad (19)$$

From (19), we can find the ACE signal. Using the ACE signal and other variables, the β value can be estimated for corresponding execution period. Since the value of β vary according to system condition, so these system parameters have to be updated regularly using a recursive least square algorithm. Fig. 4(b) shows the estimated and calculated value of β over 50 s of area-1. As depicted, for this simulation, the βcal is set to −10 B of the target control area. The parameter βest converges rapidly to the βcal .

IV. RESULTS AND DISCUSSION

In this section, a four-area power system (see Fig. 1) coupled via communication network as SG is simulated with an intelligent controller. Due to packet loss, induced network delay, the CT of SG changes, and, hence, the dynamic performance of the power system degrades. With CT changes, the MSE of system states are computed to evaluate the dynamic performance of the system. The system parameter of the four-area power system in this study is considered from [5].

MSE of Power System States

In this section, the MSE of power system states are computed. In order to validate the system dynamic performance and stability over the communication network, MSE of power system states can be computed

$$xi = [\Delta fi\ \Delta Pti\ \Delta Pgi\ \Delta P\text{tie}\ ij\ ]$$

$$\text{MSE}(k) = \{(x(k) - x0\ (k))T\ (x(k) - x0\ (k))\}$$

where $x0\ (k)$ is the nominal state of the power system at kth time, and $x(k)$ is the system state when a communication infrastructure is used. The sampling period is considered as 0.01 s. The initial value of frequency deviation for studied system is considered as 0.5 Hz. The perfect CT (case A) (see Fig. 2(a)) is selected in analysis as a reference while computing the MSE of state vector for other areas. Furthermore, the impact of CT changes on the dynamic performance of the four-area power system using MAS technique is analyzed and compared with suboptimal control designed. It is clear that CT mode is highly random as time progresses. The MSE of state variables for five imperfect CT with respect to perfect CT for area-1 is illustrated in Fig. 7(a).Furthermore, the MSE of state variables of other area with respect to perfect CT for area-2 to area-4 is illustrated in Fig. 7(b) to (d).

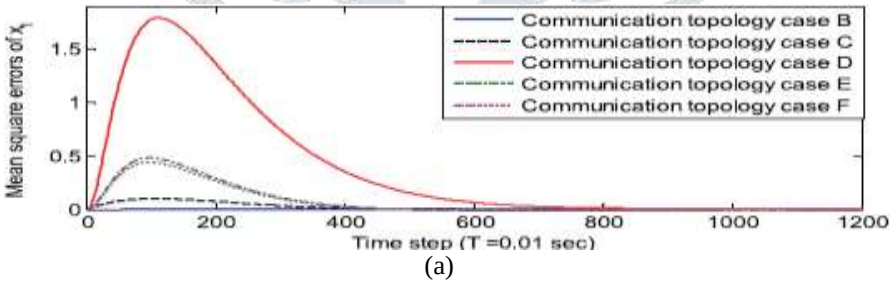

(a)

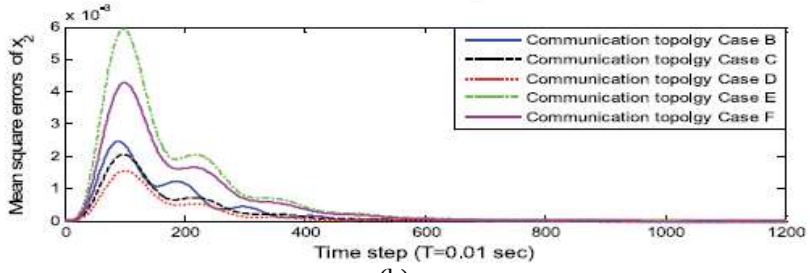

(b)

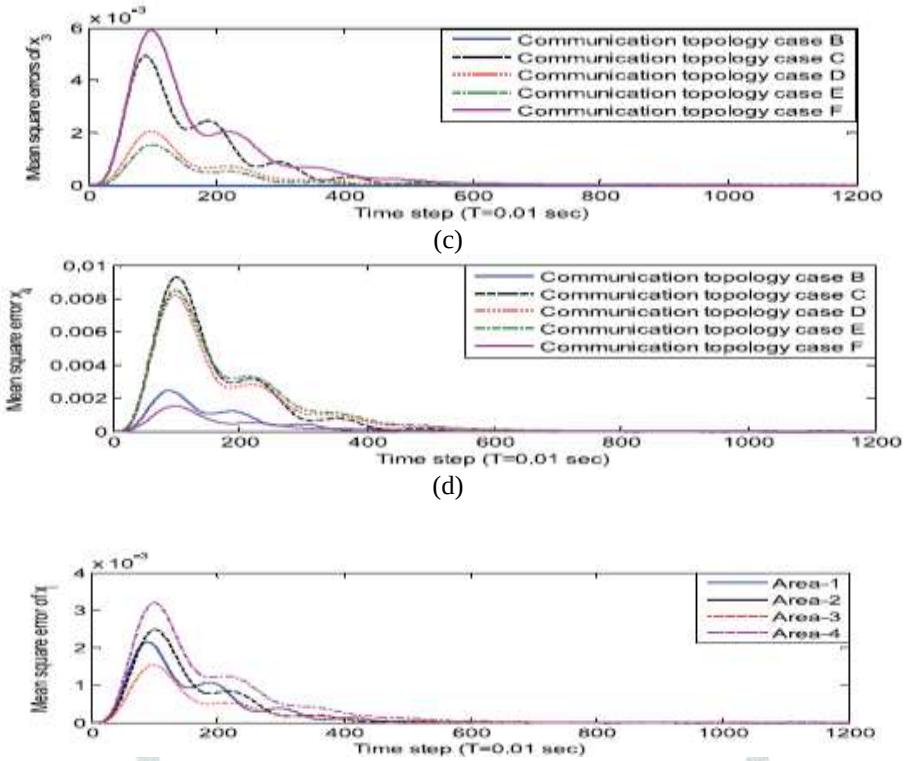

(c)

(d)

(e)

Fig. 7. Dynamic response of states and all areas MSE with MAS technique.
(a) suboptimal control design by [12]. (b) Dynamic performance of area-2.
(c) Dynamic performance of area-3. (d) Dynamic performance of area-4.
(e) Dynamic performances of all area.

The accuracy of these states seeks importance in providing information to AGC control center, on how the others areas communicate to its neighboring areas using an MAS technique. The comparative variations of MSE for state *xi* all the four areas are shown in Fig. 7(b). It may be ascertained that system parameters and bias coefficient have influence on the computation of MSE values.

REFERENCES

[1] S. K. Pandey, S. R. Mohanty, and N. Kishor, 2013. "A literature survey on load-frequency control for conventional and distribution generation power system," *Renew. Sustain. Energy Rev.*, vol. 25, pp. 318–334.

[2] C.-K. Zhang, L. Jiang, Q. H. Wu, Y. He, and M. Wu, Nov. 2013 "Further results on delay-dependent stability of multi-area load frequency control," *IEEETrans. Power Syst.*, vol. 28, no. 4, pp. 4465–4474.

[3] V. Singh, N. Kishor, and P. Samuel, May 2016 "Communication time delay estimation for load frequency control in two-area power system," *Ad Hoc Netw.*, vol. 41, no. 1, pp. 69–85.

[4] M. Erol-Kantarci and H. T. Mouftah, 2015 "Energy-efficient information and communication infrastructures in the smart grid: A survey on interactions and open issues," *IEEE Commun. Surv. Tuts.*, vol. 17, no. 1, pp. 179–197.

[5] S. Liu, X. P. Liu, and A. E. Saddik, 2014 "Modelling and distributedgain scheduling strategy for load frequency control in smart grids with communication topology changes," *ISA Trans.*, vol. 53, no. 2,pp. 454–461.

[6] V. Singh, N. Kishor, and P. Samuel, May 2015 "Impact of communication delay on frequency regulation hybrid power system using optimized H-Infinity controller," IETE journal of reasearch

[7] S. Wang, X. Men, and T. Chen, 2012 "Wide-area control of power systems through delayed network communication" *IEEE Trans. Control Syst. Technol.*, vol. 20, no. 2, pp. 495–503 .

[8] V. P. Singh, N. Kishor, and P. Samuel, 2017 "Distributed Multi-Agent System-Based Load Frequency Control for Multi-Area Power System in Smart Grid," *IEEE Trans on Industrial Electronics, Vol. 64, No. 6.*

[9] H. Bevrani, F. Daneshfar, and T. Hiyama, 2012 "A new intelligent agent based AGC design with real-time application," *IEEE Trans. Syst., Man, Cybern. C, Appl. Rev.*, vol. 27, no. 2, pp. 994–1002.

[10] T. P. I. Ahamed, P. S. N. Rao, and P. S. Sastry,2002 "A reinforcement learning approach to automatic generation control,"*Elect. Power Syst. Res.*, vol. 63, pp. 9–26.